Wildfire Spread Prediction and Assimilation for FARSITE using Ensemble Kalman Filtering[*]

Thayjes Srivas[1], Tomàs Artés[2], Raymond A. de Callafon[3], and Ilkay Altintas[4]

[1] Dept. of MAE, University of California, San Diego, U.S.A. tsrivas@eng.ucsd.edu
[2] Autonomous University of Barcelona, Spain tomas.artes@e-campus.uab.cat
[3] Dept. of MAE, University of California, San Diego, U.S.A. callafon@ucsd.edu
[4] SDSC, University of California, San Diego, U.S.A. altintas@sdsc.edu

Abstract

This paper extends FARSITE (a software used for wildfire modeling and simulation) to incorporate data assimilation techniques based on noisy and limited spatial resolution observations of the fire perimeter to improve the accuracy of wildfire spread predictions. To include data assimilation in FARSITE, uncertainty on both the simulated fire perimeter and the measured fire perimeter is used to formulate optimal updates for the prediction of the spread of the wildfire. For data assimilation, fire perimeter measurements with limited spatial resolution and a known uncertainty are used to formulate an optimal adjustment in the fire perimeter prediction. The adjustment is calculated from the Kalman filter gain in an Ensemble Kalman filter that exploits the uncertainty information on both the simulated fire perimeter and the measured fire perimeter. The approach is illustrated on a wildfire simulation representing the 2014 Cocos fire and presents comparison results for hourly data assimilation results.

Keywords: Wildfire, Data Assimilation, FARSITE, Ensemble Kalman Filter

1 Introduction

As wildfire occurrence has increased over the last several decades, so too has interest in the modeling of wildfire behavior. Wildfire modeling involves the numerical simulation of wildfires in order to understand the properties and predict the fire behavior. A software widely used for this purpose by the U.S Forest Service and other federal and state agencies is FARSITE [8]. While FARSITE's rate of fire spread model is sophisticated, it should be noted that it does not incorporate any stochastic aspects when simulating the actual wildfire. Simulations in FARSITE, under a given set of inputs and parameters and without the probabilistic generation of embers, is largely a deterministic process. FARSITE also does not possess any features for incorporating noisy and finite spatial resolution measurements of the fire perimeter during the simulation and thus has no data assimilation capabilities.

The use of data assimilation techniques in wildfire spread models is an active field of research [13, 14]. Due to the highly large-scale spatial-temporal simulations required in wildfire simulation, merging simulations and measurements may use Monte Carlo methods for data assimilation techniques [23]. Other approach provided detailed models of the wildfire in interaction with the atmosphere [12] where Tikhonov regularization is used to avoid nonphysical states. Some of the most recent data assimilation techniques for wildfire spread prediction [18, 17] heavily rely on Ensemble Kalman filtering [7, 9, 3, 11] also use in many earth science applications [6]. Although most of these methods can assimilate gridded data, the use of noisy and finite spatial resolution measurements via the explicit incorporation of uncertainty in both the simulate and measured fire perimeter for optimal adjustment of the predicted fire perimeter is often overlooked. Existing methods use a fixed dimension of the state, representing a finite number of points on the fire perimeter, during the assimilation process. The methodology in this paper allows the dimension of the state to increase, improving resolution of fire perimeters that tend to grow larger in size over time.

The aim of this paper is to include data assimilation on the fire perimeters in FARSITE via standard ensemble averaging and optimal adjustments via Kalman filter computations. Uncertainty on both the simulated fire perimeter and the measured fire perimeter is used to formulate optimal updates for the prediction of the spread of the wildfire. For that purpose, the estimate of the initial fire perimeter is augmented with a confidence region that is characterized by a covariance matrix. Ensemble sampling based on the mean and covariance information is then used to propagate the uncertainty through FARSITE for a stochastic update of the wildfire spread simulation. Although FARSITE also allows for the use of adjustment factors to alter wildfire spread for different fuel types [5], only adjustment on fire perimeters are used. Fire perimeter measurements with limited spatial resolution and a known uncertainty are used to to formulate an optimal adjustment in the fire perimeter prediction. The adjustment is calculated from the Kalman filter gain in an Ensemble Kalman filter that exploit the uncertainty information on both the simulated fire perimeter and the measured fire perimeter.

2 FARSITE

2.1 Forward Model for Wildfire Simulations

FARSITE [8], largely based on Rothermel's model [19], is widely used by the U.S. Forest Service as an effective tool of simulating the growth of natural fires in wilderness areas. It can be seen as a dedicated forward-prediction model taking the form of equation 1 which uses spatial and temporal information on the parameters θ_k and driving inputs u_k to predict a fire perimeter on a two-dimensional plane, denoted by $\bar{x}_{k+1|k}$.

$$
\begin{aligned}
\hat{x}_{k+1|k} &= f(\hat{x}_{k|k}, \theta_k, u_k) \\
\hat{y}_{k+1|k} &= C_{k+1}\hat{x}_{k+1|k}
\end{aligned}
\tag{1}
$$

For the considered wildfire data assimilation, the (measured) output y_{k+1} refers to a spatially downsampled (coarse) measurement of the actual fire perimeter, whereas wildfire related parameters θ_k may include topography and fuel parameters, and driving input u_k can refer to weather and wind conditions.

The FARSITE function $f(\cdot)$ in (1) is an implicit and high dimensional forward model that models fire growth via a vector approach and includes fire behavior models for surface fire spread [19], crown fire initiation [22], crown fire spread [20] and dead fuel moisture [4, 15]. Furthermore, the dimension n_k of the two-dimensional perimeter $\hat{x}_{k-1|k-1} \in {}^{2n_{k-1}}$ typically

changes to $n_k \geq n_{k-1}$ for $\hat{x}_{k|k-1}$ over the course of the fire simulation. The implicit knowledge of the forward model $f(\cdot)$ and changing dimension of the state $\hat{x}_{k|k-1}$ makes FARSITE and ideal application candidate for ensemble based state estimation to extend FARSITE with data assimilation capabilities to improve wildfire simulation and any success in this regard will enhance the FARSITE-based data assimilation capabilities for improved wildfire simulation.

2.2   FARSITE data inputs

FARSITE requires an input parameters set that describes the environment where the wildfire is taking place. The parameters can be classified depending on variability of such values in time and/or space. The static values (which varies mostly spatially) describing the topography, are raster maps which are combined in one single file known as FARSITE landscape file. This file contains digital elevation model information as slope, elevation or aspect as well as the description of the vegetation land cover and the fuel map [1], [2], [21].

The ignition boundary is introduced into FARSITE in a vectorial file format. In such vectorial format, some input parameters as the fire line intensity(FLI) and the rate of spread(ROS) for each point of the boundary are included. Finally, the time varying parameters are mostly weather values. This Linux FARSITE version uses a brief daily description of the weather except for the wind values. Those values are introduced every 10 minutes using a gridded format file. In this manner, an important parameter for wildfires as the wind could be updated frequently.

The weather information used in this work has been obtained from weather stations of the High Performance Wireless Network for Education and Research (HPWREN) [16, 10]. HPWREN allows requesting data in real time from the most near station to the centroid of the initial fire perimeter. The weather data is obtained in XML format and the request is parsed and written for FARSITE.

3   Ensemble Kalman Filter with FARSITE

The Ensemble Kalman Filter (EnKF) [7] is a Monte-Carlo implementation of the Bayesian update problem. Given a probability distribution of the system (the prior) and measurement likelihood, the Bayes theorem is used to to obtain the probability distribution with the data taken into account (the posterior). The state estimate is the mean of the posterior distribution. The data likelihood is the conditional probability distribution of the measurement given the current state. The EnKF assumes a Gaussian Distribution for the state variables implying that the state can be entirely characterized by the mean and the covariance of the ensemble.

3.1   Forward simulations

Unlike the Kalman Filter which uses linear equations to propagate the mean and covariance in time, the EnKF propagates the uncertainty by advancing each ensemble member through the forward model. This advantage of the EnKF provides an incentive to use it in high spatial-temporal simulations such as the FARSITE simulation software. For a brief overview of using the EnKF in FARSITE, consider the following computational steps [9]:

1. Initialize the distribution by defining a mean and a covariance of the state.

$$x_{k|k} \sim (\bar{x}_k, P_{k|k}^x), \quad x_{k|k} \in R^{n_k}.$$

2. Generate the ensembles by sampling from this distribution.

$$X_{k|k} = (x^1_{k|k}, x^2_{k|k}, x^3_{k|k}, .., x^N_{k|k}), \quad X_{k|k} \in R^{n_k \times N}$$

We now define the ensemble perturbation/error matrix $E_{x_{k|k}}$

$$E^x_{k|k} = (x^1_{k|k} - \bar{x}_k, x^2_{k|k} - \bar{x}_k, x^3_{k|k} - \bar{x}_k, ..., x^N_{k|k} - \bar{x}_k), \quad E^x_{k|k} \in R^{n_k \times N} \tag{2}$$

3. Advance each ensemble member through the forward model (FARSITE)

$$x^i_{k+1|k} = f(x^i_{k|k}, u_k), \quad i = 1, 2, \ldots, N, \quad x_{k+1|k} \in R^{n_{k+1}} \tag{3}$$

4. Calculate the mean and sample covariance of the forward ensemble. The mean is calculated simply by taking an average of the members of the forward ensemble. The sample covariance can be calculated using the forward ensemble error matrix, $E^x_{k+1|k}$, which can be calculated similar to (2), replacing $x_{k|k}$ by $x_{k+1|k}$:

$$\bar{x}_{k+1|k} = \frac{1}{N} \sum_{i=1}^{i=N} x^i_{k+1|k}$$
$$P^x_{k+1|k} = \frac{1}{N-1} E^x_{k+1|k}(E^x_{k+1|k})^T$$

We will now shortly describe how the above variables and steps are defined and carried out in a wildfire data and assimilation context using FARSITE. The mean $\bar{x}_{0|0}$ at $k = 0$ is the state which describes the ignition boundary (initial fire perimeter) in eastern e_i and northern n_i coordinates

$$\bar{x}_{0|0} = \begin{bmatrix} e_1 & n_1 & e_2 & n_2 & \cdots & e_m & n_m \end{bmatrix}^T \tag{4}$$

where (e_j, n_j) is the jth coordinate of the ignition boundary and $n^0_{0|0} = 2m$ is the dimension of the state variable $\bar{x}_{0|0}$. Let (e_c, n_c) indicate the centroid of the ignition boundary in eastern/northern coordinates, then the covariance of the state $P^x_{0|0}$ at $k = 0$ is the matrix

$$P^x_{0|0} = AP^{x_c}_{0|0}A^T + P^{\bar{x}}_{0|0} \tag{5}$$

where $P^{x_c}_{0|0}$ is the 2×2 covariance matrix for the center point $x_c = [e_c \ n_c]^T$ and $P^{\bar{x}}_{0|0}$ is the $n^0_{0|0} \times n^0_{0|0}$ covariance matrix of the state $\bar{x}_{0|0}$. The matrix A is a $n^0_{0|0} \times 2$ transformation matrix that relates $\bar{x}_{0|0}$ to the vector $x_c = [e_c \ n_c]^T$ via $\bar{x}_{0|0} = A[e_c \ n_c]^T$.

Describing the initial state covariance matrix as in (5) allows us to maintain the overall shape and size of the ignition boundary while still giving us freedom to impose a large uncertainty on the actual location of the ignition boundary via a covariance matrix $P^{x_c}_{0|0}$ on the center point $x_c = [e_c \ n_c]^T$. Having defined the initial mean and covariance matrix, step 2 is implemented by simply sampling from a normal distribution described by tits mean and covariance. Each of the ensemble members $x^i_{k|k}$ constitutes an independent ignition boundary which is used to compute an update ensemble $x^i_{k+1|k}$ through a forward model (FARSITE) simulation. The simulations in (3) can be carried out in parallel n order to increase computational speed. Note that each of the runs use the same parametric and input conditions during the FARSITE simulation.

3.2   Fire Perimeter Adjustment Using Observations

The output perimeters $x_{k+1|k}^i$ obtained from the forward model (FARSITE) simulation constitute the members of the forward/forecasted ensemble. These forward perimeters are generally vectors with a size different and larger than the initial size $n_{0|0}^0$. Furthermore, at each time time step $k+1$, the output perimeters $x_{k+1|k}^i$ may even have different sizes $n_{k+1|k}^1, n_{k+1|k}^2, \ldots, n_{k+1|k}^N$ depending on the ensemble $x_{k|k}^i$ used to compute $x_{k+1|k}^i$. To allow state updates with the EnKF approach for a varying state dimension, each new output perimeters $x_{k+1|k}^i$ is re-interpolated in 2D (eastern/northern) to a new size

$$n_{k+1|k} = \max(n_{k+1|k}^1, n_{k+1|k}^2, \ldots, n_{k+1|k}^N)$$

in order to preserve resolution at each time step $k+1$. Finally the mean $\bar{x}_{k+1|k}$ and sample covariance $P_{k+1|k}^x$ are calculated using the interpolated output perimeters of the forward ensemble and allow us to continue the computational steps for data assimilation as follows.

5. We now define the distribution of observations with a mean, $y_{k+1} \in R^m$ and the observation covariance matrix, $V_{k+1} \in R^{m \times m}$ and generate the ensemble of observations by sampling from this distribution:

$$Y_{k+1|k} = (y_{k+1|k}^1, y_{k+1|k}^2, ..., y_{k+1|k}^N), \quad Y_{k+1|k} \in R^{m \times N}$$

and the ensemble of perturbations/error for the observations:

$$E_{k+1|k}^y = (y_{k+1|k}^1 - y_{k+1}, y_{k+1|k}^2 - y_{k+1}, ..., y_{k+1|k}^N - y_{k+1}), \quad E_{k+1|k}^y \in R^{m \times N}$$

The sample covariance of the observations and sample cross covariance between the state and observations can now be calculated via

$$
\begin{aligned}
P_{k+1|k}^y &= \frac{1}{N-1} E_{k+1|k}^y (E_{k+1|k}^y)^T \\
P_{k+1|k}^{xy} &= \frac{1}{N-1} E_{k+1|k}^x (E_{k+1|k}^y)^T
\end{aligned}
$$

6. The Kalman gain is now calculated using the above computed sample covariances

$$K_{k+1} = P_{k+1|k}^{xy} (P_{k+1|k}^y)^{-1}$$

7. The next step is the update step given by

$$x_{k+1|k+1}^i = x_{k+1|k}^i + K_{k+1}(y_{k+1}^i - C_{k+1} x_{k+1|k}^i)$$

$$\bar{x}_{k+1|k+1} = \frac{1}{N} \sum_{i=1}^{i=N} x_{k+1|k+1}^i$$

where $y_{k+1}^i = y_{k+1} + v_{k+1}^i$ and y_{k+1} is the actual (noisy and downsampled) observation of the fire perimeter and v_{k+1}^i is a zero mean random variable with $N \sim (0, V_{k+1})$.

8. Finally the updated sample covariance is calculated using the ensemble of the updated state via

$$P_{k+1|k+1}^x = \frac{1}{N-1} E_{k+1|k+1}^x (E_{k+1|k+1}^x)^T$$

where, $E_{k+1|k+1}^x$ is again similar to (2) with $x_{k+1|k+1}$ replaced by $x_{k+1|k}$ and $\bar{x}_{k+1|k+1}$ replaced by $\bar{x}_{k|k}$. At any time instant, the estimate of the state, $\hat{x}_{k+1|k+1}$, is the mean of the ensemble, $\bar{x}_{k+1|k+1}$.

For the continued iteration along the time index k, one replace $k \to k+1$ and repeat steps 2 to 8. The above steps can be described in context for wildfire data assimilation. It is clear that y_{k+1} in in step 5 is defined as the downsampled version of the "true" fire perimeters given by $y_{k+1} = C_{k+1}x_{k+1}$ where C_{k+1} is the spatial downsampling matrix and x_{k+1} is the true (yet unknown) state data of the fire perimeter.

At this step we also introduce the observation covariance matrix V_{k+1}. In the wildfire context, this characterizes the variance on our measurements of the fire perimeters y_{k+1}. The mean and covariance matrix of the observations allows us to apply uncertainty on our measurements which is very important in calculating the Kalman gain K_{k+1} in step 6. In the next step we update each of our interpolated perimeters, $x^i_{k+1|k}$ which we obtained from the output of the FARSITE, using the Kalman gain and a sample measurement from the ensemble of observations. The ensemble of observations is characterized by its mean y_{k+1} and covariance matrix V_{k+1} described earlier. These updated perimeters $x^i_{k+1|k+1}$ are the fire perimeters which will be used to resume our simulation from the $k+1$th time step. In the remaining steps we do a similar calculation as in the first 4 steps and obtain the updated mean of the fire perimeters $\bar{x}_{k+1|k+1}$ and the updated sample covariance matrix $P^x_{k+1|k+1}$.

4   Application in WildFire Data Assimilation

4.1   Reference Data for Simulation

In this section we collect topography data and weather conditions from the May 2014 Cocos Fire in San Marcos and use this to generate parametric conditions and input data for a FARSITE wildfire simulation. These parametric conditions and input data are used to produce the "true" fire perimeters x_{k+1} that will be used as a reference for the performance evaluation of the data assimilation tools in this paper. The simulated fire perimeters are depicted in Fig. 1 over a 18 hour time period with a one hour time resolution and a 90m spatial resolution along the perimeter, starting from a given square 30m×30m ignition boundary x_0 at $t = k = 0$.

For testing the data assimilation tools, the "true" data with a 90m spatial resolution along the perimeter is down-sampled to generate the output y_{k+1} by

$$y_{k+1} = C_{k+1}x_{k+1} + v_{k+1},$$

where C_{k+1} is a downsampling matrix, and measurements y_{k+1} are produced at a spatial resolution of only 360m along the perimeter. The measurements are perturbed by a white noise v_{k+1} with a standard deviation of 50m. In addition, it is assumed that the ignition boundary x_0 is not known at the start of the data assimilation procedure. Instead, an initial estimate $\hat{x}_{0|0} \neq x_0$ along with a covariance matrix is used.

4.2   Forward Simulation Without Data Assimilation

To illustrate the need for data assimilation, a forward simulation from FARSITE is initialized at $\hat{x}_0 \neq x_0$. The ignition boundary (initial fire perimeter) $\hat{x}_0$ is also characterized by a square 30×30m fire perimeter, but with the center of the perimeter 215m off in eastern direction and 730m off in in northern direction compared to the "true" x_0. A side-by-side comparison can be made between the reference data (the "true" fire perimeters) x_{k+1} in Fig. 1 and the fire perimeters $\hat{x}_{k+1}$ obtained by the forward simulation from FARSITE initialized at $\hat{x}_0 \neq x_0$ in Fig. 2. It is clear that the relatively small initial error due to $\hat{x}_0 \neq x_0$ between the initial fire perimeters leads to a growing divergence of the fire perimeters over time.
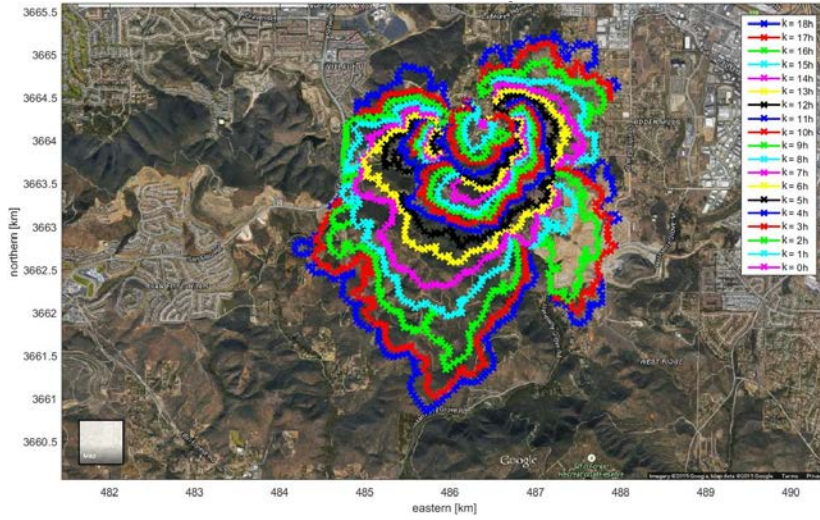
Figure 1: Noise free reference data of the "true" hourly fire perimeters x_k starting at x_0 over a 18 hour time period and a spatial resolution of 90m along the fire perimeters. A noise perturbed and down-sampled measurement y_k of this data with a spatial resolution of 360m along the perimeter is used for data assimilation.
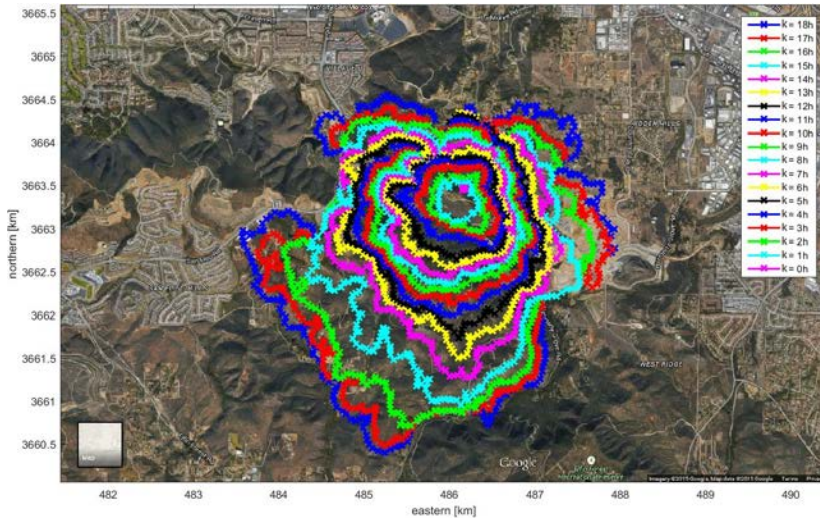

Figure 2: Forward (FARSITE) simulation of hourly fire perimeters $\hat{x}_k$ over a 18 hour time period with a spatial resolution of 90m along the fire perimeters started at an off-set initial fire perimeter $\hat{x}_0 \neq x_0$.

The diverging error can be characterized via the Root Mean Square (RMS) error

$$E_{rms_k} = \left(\frac{\sum_{i=1}^{i=n_k} (x_k - \hat{x}_k)^2)}{n_k} \right)^{1/2} \tag{6}$$

where n_k is the state size, representing the number of points on the fire perimeter. Evaluating the RMS error for the forward simulation of hourly fire perimeters $\hat{x}_k$ shown earlier in Fig. 2, leads to the progress of the RMS error summarized in Fig. 3. It is clear from this figure that a simple forward simulation with FARSITE, without the corrections provided by data assimilation, does not improve the RMS error and eventually leads to a diverging RMS error. Data assimilation is needed to stabilize the RMS error and correct for the initial error in the fire perimeter $\hat{x}_0 \neq x_0$.
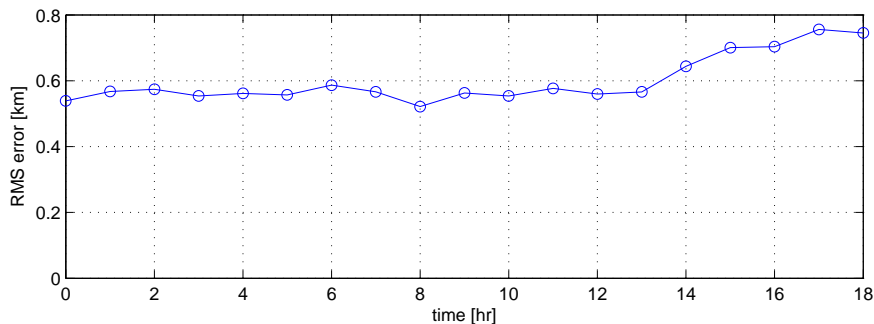

Figure 3: RMS error of hourly fire perimeters $\hat{x}_k$ computed via forward (FARSITE) simulation started at an off-set initial fire perimeter $\hat{x}_0 \neq x_0$.

4.3   Data Assimilation with Hourly Updates

Using noisy and down-sampled measurements y_{k+1} at time index $k+1$, an estimate $\hat{x}_{k+1|k+1}$ is formulated of the "true" fire perimeter x_{k+1} via the ensemble Kalman filter (EnKF) approach outlined earlier in Section 3. To initialize the data assimilation procedure, the same inaccurate value of the initial fire perimeter $\hat{x}_{0|0} \neq x_0$ will be used, where $\hat{x}_{0|0}$ is a square 30×30m fire perimeter, but with the center of the perimeter 215m off in eastern direction and 730m off in in northern direction.

As each point on the fire perimeter consists of a eastern and northern coordinate, the initial square fire perimeter of 4 perimeter points requires an 8 dimensional state estimate $\hat{x}_{0|0}$. The ensembles are created using an 8×8 covariance matrix $P^{\bar{x}}_{0|0}$ for the mean $\bar{x}_{0|0} = \hat{x}_{0|0} \neq x_0$ and a 2×2 covariance matrix $P^{x_c}_{0|0}$ for the center x_c of the square ignition boundary. The covariance matrices are given by

$$P^{\bar{x}}_{0|0} = diag\{P, P, P, P\}, \quad P = \begin{bmatrix} 5 & 0 \\ 0 & 5 \end{bmatrix}, \quad P^{x_c}_{0|0} = \begin{bmatrix} 150 & 0 \\ 0 & 150 \end{bmatrix}$$

and indicate a relative large uncertainty on the center point and a smaller uncertainty on the individual corner points of the square ignition boundary. The covariance information is combined via (5) to get the complete initial covariance matrix $P^x_{0|0}$ to create initial ensembles $x^i_{0|0}, \ i = 1, 2, \ldots, N$ that are advanced through the forward model (FARSITE) in (3) where $N = 100$.

During the subsequent steps of the EnKF method outlined in Section 3, the comparison of the updated perimeter and the perimeter of the reference fire along with a confidence region on one of the coordinates of the reference fire is depicted in Fig. 4. It can be observed that the predicted and reference fire perimeter converge fairly quickly. This is also confirmed by the plot

of the RMS Error convergence rate for this simulation in Fig. 5. Clearly the error decreases by a very large amount in the first update and then decreases by only small amounts in subsequent updates, showing the quick convergence and effectiveness of the data assimilation technique to account for errors in the initial fire perimeter.
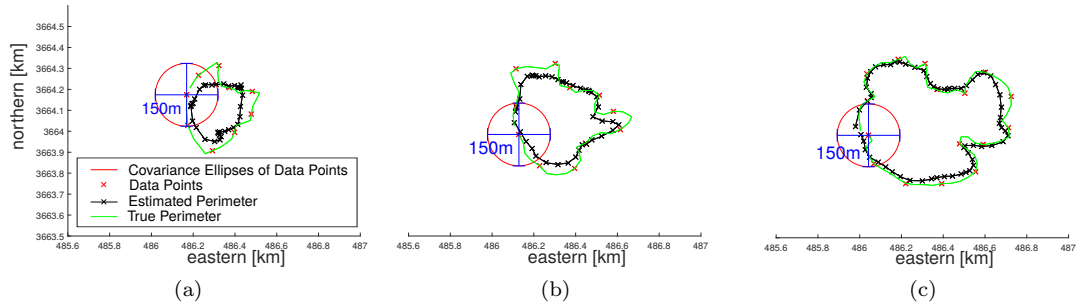

(a)   (b)   (c)

Figure 4: Comparison of Updated Perimeter $\hat{x}_{k|k}$ and Reference Perimeter x_k for time steps (a) $k = 1$ (b) $k = 2$ and (c) $k = 3$. The circles indicate the 99% confidence interval (3 times standard deviation of 50m or variance of 2500m^2) of the observations.
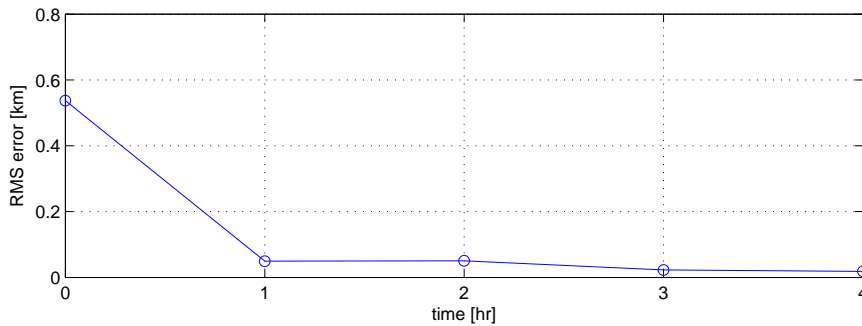

Figure 5: RMS Error Between the Updated Perimeters $\hat{x}_{k|k}$ and the "true" Fire Perimeters x_k with hourly updates and a measurement variance of 2500m^2. It is assumed the first measurement and data assimilation update is performed at $k = 1$.

4.4   Effect of Measurement Uncertainty on Convergence Rate

For the hourly updates, the convergence was shown to occur in only a single update step of the EnKF algorithm, despite the error on the initial fire perimeter. The fast convergence is due to the relatively large covariance on the initial fire perimeter and relatively small covariance on the fire perimeter observations. Next we investigate the effect of varying this uncertainty in the measurements of the reference fire perimeter on the convergence rate. The simulation is initialized with a smaller initial uncertainty to see a more pronounced effect of this variation. We apply the same covariance matrix on the coordinates of the mean perimeter and then give a smaller 2×2 covariance matrix for the center of the ignition boundary compared to the previous

simulation.

$$P_{0|0}^{\bar{x}} = diag\{P, P, P, P\}, \quad P = \begin{bmatrix} 5 & 0 \\ 0 & 5 \end{bmatrix}, \quad P_{0|0}^{x_c} = \begin{bmatrix} 50 & 0 \\ 0 & 50 \end{bmatrix}$$

For the first simulation we update the perimeters with a time resolution of 1 hour but with measurements, $y_{k+1} + v_{k+1}^{50}$, where v_{k+1}^{50} is zero mean white noise with 2500m^2 variance. Whereas for the second simulation we use noisier measurements, $y_{k+1} + v_{k+1}^{200}$, where v_{k+1}^{200} is zero mean white noise with a 40000m^2 variance. A comparison of the respective RMS progression curves can be found Fig. 6.
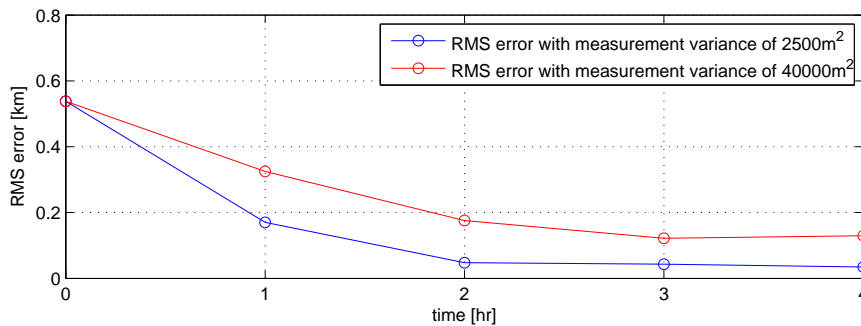

Figure 6: Comparison of RMS Errors between data assimilation using measurements of 2500m^2 variance and measurements of 40000m^2 variance

From Fig. 6 we can clearly see that the simulation that uses fire perimeter observations with a 40000m^2 variance would take a larger number of steps to converge to the same error when compared to the simulation which uses more accurate fire perimeter observations with a 2500m^2 variance.

4.5   Data Assimilation with Reduced Update Frequency

To complete the analysis of the EnKF filter for data assimilation performance, we repeat the procedure with the same initial fire perimeter and covariance matrices as used in the simulation presented in Section 4.3. For performance evaluation we now plot the (mean) RMS Error *and* the variance of the RMS Error during the course of the simulation. In this case the assimilation steps occur do not occur hourly, but are further apart. Compared to Figure 4, data assimilation is only done at the time steps $k = 1$ and $k = 4$ instead of every hourly time step. The results in Figure 7 show the effect of both the mean and variance of the RMS error and indicate a significant drop in the mean RMS error and its variance whenever a data assimilation step is performed. Even though the mean RMS error does not increase considerably when no data assimilation step is performed, the uncertainty does increase significantly during time steps without data assimilation. This large uncertainty in the RMS error informs us that even though the (mean) RMS error itself may remain small between the reference and offset perimeters, the uncertainty on the fire perimeter may grow without frequent data assimilation steps.
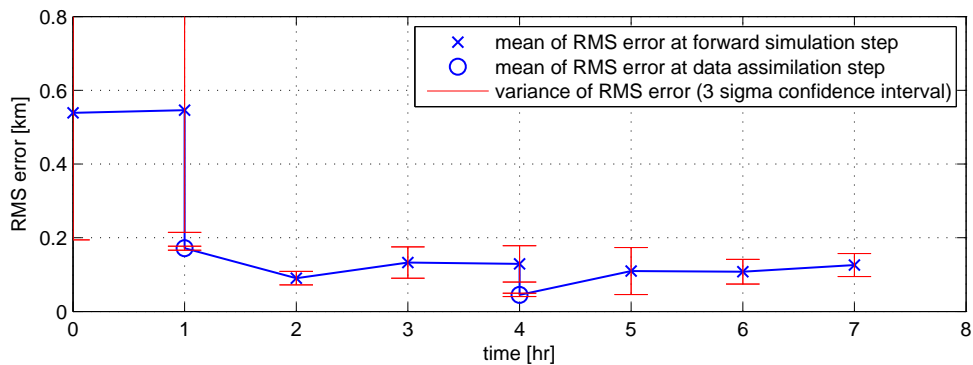
Figure 7: Progress in mean RMS Error and variance of RMS Error when data assimilation steps are performed only at the time steps $k = 1$ and $k = 4$ hours.

5   Conclusions and Future Work

Data assimilation in FARSITE is accomplished by characterizing both simulated and actual measured fire perimeter with a mean and covariance matrix (confidence regions) to formulate optimal updates for the prediction of the spread of the wildfire. Optimal updates are computed via a fire perimeter adjustment, weighted by a Kalman filter gain that is computed via an Ensemble Kalman filter approach. Application of the proposed FARSITE data assimilation to a wildfire simulation representing the 2014 Cocos fire confirmed an inverse relation between the rate of convergence of the fire perimeter and the uncertainty on the fire perimeter measurements. In the presence of incorrect ignition boundary, it is shown that convergence to the actual wild fire perimeter is obtained in only a few data assimilation steps in case of a relatively small (50m) standard deviation on the measured fire perimeters measured at a resolution of 360m. The simulation study also includes results on convergence for larger uncertainty in the measured fire perimeters and when data assimilation steps are not performed regularly. State updates only involved the fire perimeter and future work will extend this to fuel adjustment factors used in FARSITE to account for wildfire spread variations over homogeneous fuel types.

References

[1] F.A. Albini. Estimating wildfire behavior and effects. Technical Report GTR-INT-30, Dept. of Agriculture, Forest Service, Intermountain Forest and Range Experiment Station, Ogden, UT, 1976.

[2] H. E. Anderson. Aids to determining fuel models for estimating fire behavior. Technical Report GTR-INT-122, U.S. Dept. of Agriculture, Forest Service, Intermountain Forest Range and Experiment Station, Ogden, UT, 1982.

[3] J.D. Beezley and J. Mandel. An ensemble Kalman-particle predictor-corrector filter for non-gaussian data assimilation. *Lecture Notes in Computer Science*, 5545:470–478, 2009.

[4] L.S Bradshaw, J.E. Deeming, R.E. Burgan, and J.D. Cohen. The 1978 national fire-danger rating system: technical documentation. Technical Report GTR-INT-169, U.S. Dept. of Agriculture, Forest Service, Intermountain Forest and Range Experiment Station, Ogden, UT, 1984.

[5] J. Brakeall. Wildfire assessment using FARSITE fire modeling: A case study in the chihuahua desert of mexico. Master's thesis, Florida International University, 2013.

[6] G. Evensen. The ensemble Kalman filter: theoretical formulation and practical implementation. *Ocean Dynamics*, 53(4):343–367, 2003.

[7] G. Evensen. *Data Assimilation: The Ensemble Kalman Filter*. Springer-Verlag, Berlin, 2009.

[8] M.A. Finney. FARSITE: Fire area simulator-model development and evaluation. Technical Report RMRS-RP-4 Revised, U.S. Dept. of Agriculture, Forest Service, Rocky Mountain Research Station, 2004.

[9] S. Gillijns, O.B. Mendoza, J. Chandrasekar, B.L.R. De Moor, D.S. Bernstein, and A. Ridley. What is the ensemble Kalman filter and how well does it work? In *American Control Conference*, pages 4448–4453, Minneapolis, MN, 2006.

[10] T. Hansen, P. Yalamanchili, and H-W Braun. Wireless measurement and analysis on HPWREN. In *Proceedings of Passive and Active Measurement Workshop*, pages 222–229, Fort Collins, CO, 2002.

[11] J. Mandel, J.D. Beezley, L. Cobb, and A. Krishnamurthy. Data driven computing by the morphing fast Fourier transform ensemble Kalman filter in epidemic spread simulations. *Procedia Computer Science*, 1:1221–1229, 2010.

[12] J. Mandel, J.D. Beezley, J.L. Coen, and M. Kim. Data assimilation for wildland fires: Ensemble Kalman filters in coupled atmosphere-surface models. *IEEE Control Systems Magazine*, 29:47–65, 2009.

[13] J. Mandel, L.S. Bennethum, M. Chen, J.L. Coen, C.C. Douglas, L.P. Franca, C.J. Johns, M. Kim, A.V. Knyazev, R. Kremens, V. Kulkarni, G. Qin, A. Vodacek, J. Wu, W. Zhao, and A. Zornes. Towards a dynamic data driven application system for wildfire simulation. *Lecture Notes in Computer Science*, 3515:632–639, 2005.

[14] J. Mandel, M. Chen, L.P. Franca, C. Johns, A. Puhalskii, J.L. Coen, C.C. Douglas, R. Kremens, A. Vodacek, and W. Zhao. A note on dynamic data driven wildfire modeling. *Lecture Notes in Computer Science*, 3038:725–731, 2004.

[15] R.M. Nelson. Prediction of diurnal change in 10-h fuel stick moisture content. *Canadian Journal of Forest Research*, 30:1071–1087, 2000. doi:10.1139/CJFR-30-7-1071.

[16] J. Otero, P. Yalamanchili, and H.-W. Braun. High performance wireless networking and weather. http://hpwren.ucsd.edu/info/images/weather.pdf, 2001.

[17] M.C. Rochoux, C. Emery, S. Ricci, B. Cuenot, and A. Trouvé. Towards predictive data-driven simulations of wildfire spread. part II: Ensemble Kalman filter for the state estimation of a front-tracking simulator of wildfire spread. *Nat. Hazards Earth Syst. Sci.*, 15, 2015.

[18] M.C. Rochoux, S. Ricci, D. Lucor, B. Cuenot, and A. Trouvé. Towards predictive data-driven simulations of wildfire spread. part I: Reduced-cost ensemble Kalman filter based on a polynomial chaos surrogate model for parameter estimation. *Nat. Hazards Earth Syst. Sci.*, 14:2951–2973, 2014.

[19] R.C. Rothermel. A mathematical model for predicting fire spread in wildland fuels. Technical Report RP-INT-115, U.S. Dept. of Agriculture, Forest Service, Intermountain Research Station, Ogden, UT, 1972.

[20] R.C. Rothermel. Predicting behavior and size of crown fires in the northern Rocky Mountains. Technical Report RP-INT-438, U.S. Dept. of Agriculture, Forest Service, Intermountain Research Station, Ogden, UT, 1991.

[21] J.H. Scott and R.E. Burgan. Standard fire behavior fuel models: a comprehensive set for use with Rothermel's surface fire spread model. Technical Report RMRS-GTR-153, U.S. Dept. of Agriculture, Forest Service, Rocky Mountain Research Station, Fort Collins, CO, 2005.

[22] C.E. Van Wagner. Conditions for the start and spread of crownfire. *Canadian Journal of Forest Research*, 7(1):23–34, 1977. 10.1139/x77-004.

[23] H. Xue, F. Gu, and X. Hu. Data assimilation using sequential Monte Carlo methods in wildfire spread simulation. *ACM Transactions on Modeling and Computer Simulation*, 22(23):1–25, 2012.